Gas Separation Hot Paper

International Edition: DOI: 10.1002/anie.201603211
German Edition: DOI: 10.1002/ange.201603211

A Highly Permeable Aligned Montmorillonite Mixed-Matrix Membrane for CO_2 Separation

Zhihua Qiao, Song Zhao, Jixiao Wang, Shichang Wang, Zhi Wang, and Michael D. Guiver**

Abstract: *Highly permeable montmorillonite layers bonded and aligned with the chain stretching orientation of polyvinylamineacid are immobilized onto a porous polysulfone substrate to fabricate aligned montmorillonite/polysulfone mixed-matrix membranes for CO_2 separation. High-speed gas-transport channels are formed by the aligned interlayer gaps of the modified montmorillonite, through which CO_2 transport primarily occurs. High CO_2 permeance of about 800 GPU is achieved combined with a high mixed-gas selectivity for CO_2 that is stable over a period of 600 h and independent of the water content in the feed.*

Carbon dioxide membrane separation processes, including CO_2 removal from syngas and natural gas[1] and CO_2 capture from flue gas for environmental remediation,[2] have attracted increasing attention owing to their lower energy consumption and operational simplicity compared with traditional separation techniques.[3] Constructing channels with high gas permselectivity in membranes is an effective approach to improve gas-separation performance. Porous materials, such as zeolites, metal–organic frameworks, and multilayered oxides (clays), are employed to fabricate gas separation membranes, as they possess non-tortuous pores with defined sizes that serve as high-speed transport channels with high permselectivity for gas molecules.[4,5]

Clays, such as montmorillonite (MT), kaolinite,[6] and hydrotalcite,[7] which have multilayered structures with interlayer exchangeability and hydroxy groups on the layered walls, have a strong affinity towards CO_2 molecules and thus have the potential to be utilized as CO_2 transport channels.[7,8]

[*] Dr. Z. Qiao, Dr. S. Zhao, Prof. Dr. J. Wang, Prof. Dr. S. Wang, Prof. Dr. Z. Wang
Chemical Engineering Research Center
School of Chemical Engineering and Technology
Tianjin University, Tianjin, 300072 (P.R. China)
and
Tianjin Key Laboratory of Membrane Science and Desalination Technology, State Key Laboratory of Chemical Engineering
Tianjin University, Tianjin 300072 (P.R. China)
E-mail: wangzhi@tju.edu.cn
Prof. Dr. M. D. Guiver
State Key Laboratory of Engines
Tianjin University, Tianjin 300072 (P.R. China)
E-mail: guiver@tju.edu.cn
Dr. Z. Qiao, Dr. S. Zhao, Prof. Dr. J. Wang, Prof. Dr. S. Wang, Prof. Dr. Z. Wang, Prof. Dr. M. D. Guiver
Collaborative Innovation Center of Chemical Science and Engineering (Tianjin), Tianjin 300072 (P.R. China)
Supporting information and the ORCID identification numbers for the authors of this article can be found under http://dx.doi.org/10.1002/anie.201603211.

Alignment of the clay interlayer gaps containing water molecules and ions enables the construction of gas-selective high-speed transport channels. To the best of our knowledge, highly permeable mixed-matrix membranes containing aligned clay layers supported on a substrate have never been reported.

MT was selected owing to its high interlayer exchangeability that allows the interlayer spacing to be readily controlled, as well as its nanoscale particle size, which is suitable for ultrathin membrane fabrication. In the present work, aligned MT (AMT) layers were anchored onto a porous polysulfone (PSf) substrate (ca. 45 nm mean pore diameter) using polyvinylamineacid as a polymer linker and an MT alignment agent. The MT framework is composed of a two-layer silica tetrahedron and a single-layer alumina octahedron.[7] Water molecules, Na ions, and small amounts of Ca and K ions reside in the interlayer gaps of MT. To avoid precipitation of Ca ions in the presence of hydroxy groups, MT was first exchanged by Na ions to form Na-exchanged MT. Then, the surface of the PSf substrate was hydroxylated and grafted with polyvinylamineacid. Finally, an AMT/PSf mixed-matrix membrane was obtained by interspersing Na-exchanged MT with polyvinylamineacid using an ethoxysilane coupling agent, 3-aminopropyltriethoxysilane. The AMT interlayer gaps are aligned along the stretching orientation of the polyvinylamineacid chains, and serve as high-speed CO_2 transport channels.

Figure 1 depicts Na and K ions residing in the Na-exchanged MT interlayer gaps, while hydroxy groups are distributed on the surface. Water molecules were removed from Na-exchanged MT by heat treatment. Na-exchanged MT has a cuboid shape with average dimensions of about 0.1 μm × 0.04 μm × 0.01 μm from the morphological and structural characterization (Figure S1; for details see the Supporting Information).

The surface of the PSf substrate was functionalized by hydroxylation using aqueous $K_2S_2O_8$ (Figure S2; for details, see the Supporting Information). Polyvinylamineacid, which contains secondary amine, carboxylic acid, and formamide groups, was prepared with an average molecular weight of 25000–30000 Da (Figures S3 and S4; see the Supporting Information for details). The molar ratio of the carboxylic acid to formamide groups in polyvinylamineacid was 1:1 according to elemental analysis. The polyvinylamineacid was grafted onto the hydroxylated PSf substrate surface at multiple points by reaction of the carboxylic acid groups in thionyl chloride solvent to give the modified PSf substrate. (Figures S5 and S6; see the Supporting Information for further details). The presence of thionyl chloride is believed to facilitate polyvinylamineacid chain stretching and uncoil-

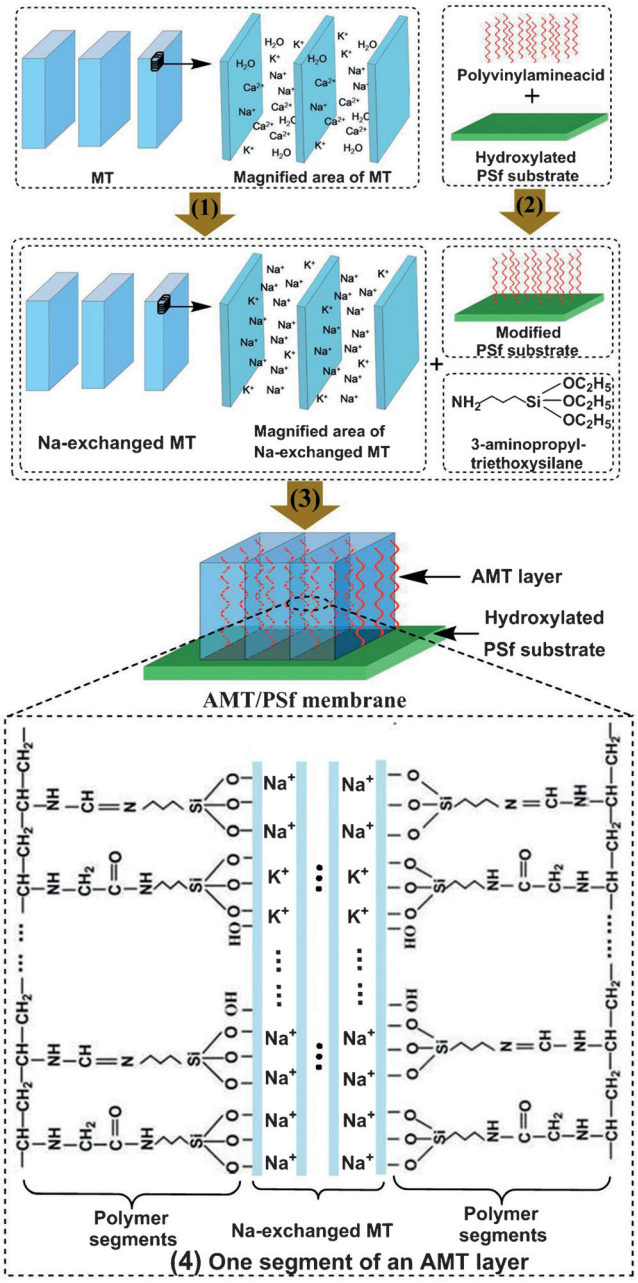

Figure 1. Formation of the AMT/PSf membrane: 1) Na ion exchange to form Na-exchanged MT; 2) surface modification by grafting polyvinylamineacid onto the hydroxylated PSf substrate to form the modified PSf substrate; 3) immobilization of Na-exchanged MT onto the modified PSf substrate through uncoiled polyvinylamineacid to obtain the AMT/PSf membrane; 4) one segment of an AMT layer.

ing because thionyl chloride converts carboxylic acid groups into acyl chlorides, which reduces the overall amount of hydrogen bonding. The mean square radius of gyration of polyvinylamineacid dissolved in thionyl chloride and grafted onto the PSf substrate was characterized by gel permeation chromatography (GPC) coupled with a low-angle laser light scattering detector, and determined to be 45 nm. Owing to the polymer chain flexibility, the polyvinylamineacid chains present a curve distribution on the PSf substrate (see the Supporting Information).

The 3-aminopropyltriethoxysilane coupling agent was used to link Na-exchanged MT with polyvinylamineacid acid. Figure 1(4) illustrates the immobilization of Na-exchanged MT onto polyvinylamineacid that had previously been grafted onto the hydroxylated PSf substrate. Amide groups and carbon–nitrogen double bonds form through the reaction of the 3-aminopropyltriethoxysilane amine groups with the polyvinylamineacid acyl chlorides and formamide groups in the presence of a condensation agent and catalyst (see the Supporting Information). The hydroxy groups in Na-exchanged MT bond by reaction with the ethoxysilane groups in the coupling agent, enabling the efficient immobilization of Na-exchanged MT interspersed with polyvinylamineacid on the modified PSf substrate. The resulting grafted AMT layers also interact through intermolecular hydrogen bonding with formamide and secondary amine groups (Figure S7). The calculated interlayer spacing of AMT is 0.88 nm, which is the same as that of Na-exchanged MT. The hydroxy group distributions on the two walls of Na-exchanged MT are identical, which indicates that both walls will be equally likely to react with the coupling agent. Similarly, uncoiled polyvinylamineacid chains with a uniform mean square radius of gyration will also be equally likely to react with the coupling agent. Therefore, the pull forces of uncoiled polyvinylamineacid chains on the two walls are almost identical, causing the Na-exchanged MT to align vertically on the PSf substrate. Figure 1 depicts the overall scheme to incorporate and align AMT layers onto a PSf substrate to prepare the AMT/PSf membrane.

To investigate the gas adsorption performance of the MT component in the AMT/PSf membrane, random MT (RMT) was synthesized (see the Supporting Information). RMT has a very similar structure to the AMT immobilized in the AMT/PSf membrane (Figure S8). Thus the gas adsorption behavior of the AMT component can be represented by that of RMT. Figure 2a shows that RMT has a regular cuboid shape with dimensions of about 0.1 μm × 0.04 μm × 0.04 μm and a similar morphology to AMT on the AMT/PSf membrane surface, but without visible defects (Figure 2b and Figure S9a). The AMT/PSf membrane and RMT were characterized by advanced transmission electron microscopy (TEM; Tecnai G2 F20, Philips, Holland). The highly orientated Na-exchanged MT anchored onto the AMT/PSf membrane is compared with RMT in Figure 2c,d. Figure S9b is a cross-sectional SEM image of the AMT/PSf membrane, showing that the AMT layer has a compacted structure with a thickness of about 0.1 μm. EDX mapping of the AMT cross-section presents a uniform distribution of the element silicon (Figure S9b). Figure 2b indicates that although cracks are observed on the surface of the AMT layer in the AMT/PSf membrane, possibly arising from the sample preparation, a thin sealant layer was formed by polyvinylamineacid under the cracks in the AMT layer (see the Supporting Information). This was confirmed by a featureless EDX surface map with a uniform distribution of nitrogen in the crack region of the AMT layer (Figure S9c).

Figure S10 shows mixed-gas isotherms for Na-exchanged MT. It can be concluded that the hydroxy groups of MT containing Na ions (or Ca ions) can reversibly interact with

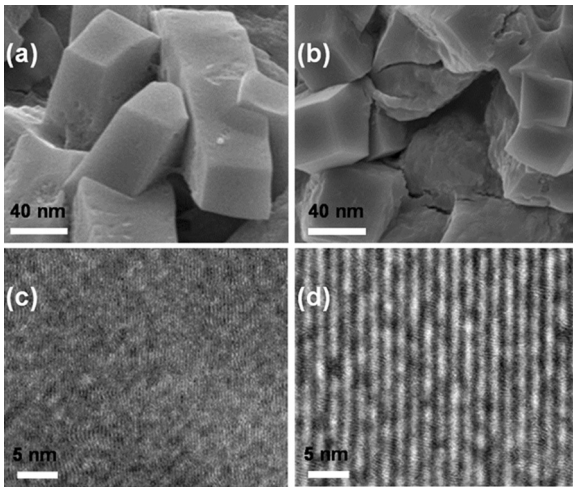

Figure 2. a) SEM image of RMT. b) Surface SEM image of the AMT/PSf membrane (visible surface cracks are likely the result of sample preparation). c) TEM image of RMT. d) Surface TEM image of the AMT/PSf membrane.

acidic CO_2 in the interlayer gaps, preferentially facilitating CO_2 transport, while restraining the adsorption of N_2, CH_4, and H_2.[8] Moreover, the appropriate width of the interlayer gaps (0.88 nm) allows for CO_2 molecular surface diffusion within the gaps.[9,10] The single-gas isotherms of RMT, shown in Figure 3, are representative of the gas adsorption performance of the AMT component in the AMT/PSf membrane. It can be deduced that CO_2, N_2, CH_4, and H_2 adsorption in the AMT interlayer gaps follows Henry's Law for a certain pressure range (see the Supporting Information).

To elucidate the gas-transport properties of the AMT/PSf membrane, comparative polyvinylamineacid/PSf, RMT/PSf, and polyvinylamineacid/Na-exchanged MT/PSf membranes were prepared (see the Supporting Information). The gas-transport properties of these membranes were determined using dried sweep gas, dried H_2, N_2, CH_4, CO_2, CO_2/N_2 mixed gas (15:85, v/v), CO_2/CH_4 mixed gas (10:90, v/v), and CO_2/H_2 mixed gas (40:60, v/v) at 50 °C (Figure S11; see the Supporting Information for further details). Gas transport through the membrane occurs mainly within the AMT interlayer gaps, because the pure-gas permeances for the AMT/PSf membrane are much higher than those of the polyvinylamineacid/PSf membrane, as shown in Figure 4.

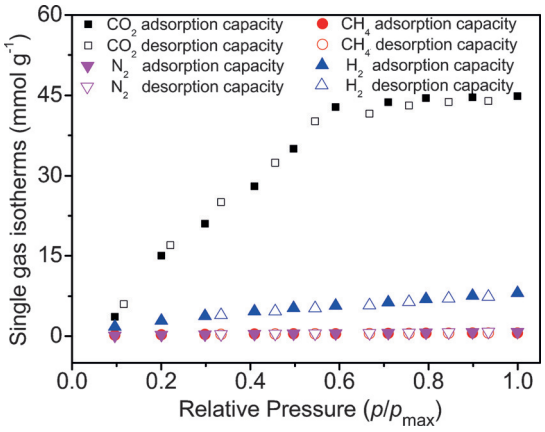

Figure 3. Single-gas isotherms of RMT, $p_{max} = 3.0$ MPa. Red circles, both filled and open, are obscured by filled and open pink triangles, respectively.

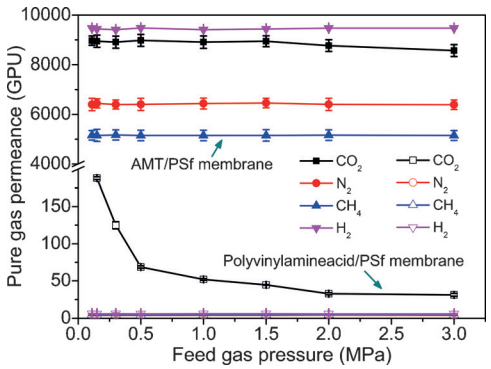

Figure 4. Comparative pure-gas permeances of AMT/PSf (filled symbols) and polyvinylamineacid/PSf membranes (open symbols).

Mixed-gas transport exhibits significantly different behavior from pure-gas transport. The mixed-gas CO_2 separation performance of AMT/PSf and comparative RMT/PSf membranes is shown in Figure 5. In the case of mixed gases, N_2, CH_4, and H_2 molecules may occupy a portion of the CO_2 transport channels and weaken the interaction between the hydroxy groups and CO_2 molecules. Given the already narrow width of the AMT interlayer gaps, the CO_2 adsorption capacity and diffusion rate in the AMT interlayer gaps are remarkably reduced, resulting in a significant decrease in the mixed-gas CO_2 permeance for the AMT/PSf membrane (Figure 5a) compared to pure gases (Figure 4). Owing to the preferential adsorption of CO_2 molecules in the AMT interlayer gaps, the N_2, CH_4, and H_2 mixed-gas permeances of the AMT/PSf membrane are much lower than the pure-gas permeances (see the Supporting Information), giving rise to much higher mixed-gas selectivities (Figure 5b). Figure 5 shows that the CO_2 permeance and permselectivity of the AMT/PSf membrane apparently do no depend on the feed pressure (see the Supporting Information). Based on the adsorption and desorption behavior of CO_2 in RMT (Figure 3), when the CO_2 feed pressure is below 1.8 MPa, the CO_2 permeance of the AMT/PSf membrane is relatively constant. At CO_2 feed pressures above 1.8 MPa, the gradient of the equilibrium concentration of CO_2 molecules in the AMT/PSf membrane decreases, resulting in a lower pure CO_2 permeance (Figure 4).

The mixed-gas CO_2 separation performance of the RMT/PSf membrane is also analyzed in Figure 5. The amount of Na-exchanged MT contained in AMT/PSf and RMT/PSf membranes with a certain effective area was similar, allowing for a valid comparison to be made (see the Supporting Information). The significantly higher gas permeance of the AMT/PSf membrane indicates a shorter gas transport pathway in the membrane owing to the alignment of Na-exchanged MT [see Equation (1) in the Supporting Informa-

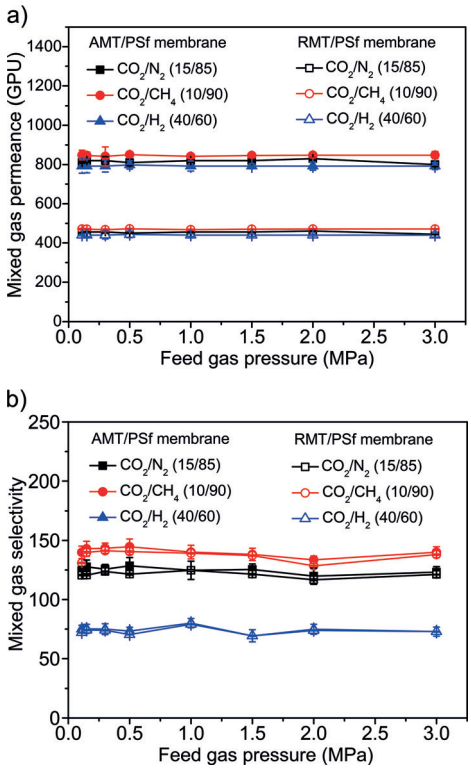

Figure 5. a) CO_2 permeance and b) selectivity of the AMT/PSf (filled symbols) and RMT/PSf (open symbols) membranes tested with gas mixtures. AMT/PSf has a much higher gas permeance than RMT/PSf, but a similar gas pair selectivity.

tion]. However, the gas pair selectivities are not influenced by the transport path lengths in RMT/PSf, based on Equation (2) in the Supporting Information. The high selectivities observed for CO_2/N_2, CO_2/CH_4, and CO_2/H_2 for the AMT/PSf membranes (Figure 5b) are indicative of defect-free selective layers, despite the appearance of surface cracks, which likely arise from sample preparation. Any defects extending through the selective layer would also be sealed with polyvinylamineacid, owing to the membrane formation method. The mixed-gas transport in polyvinylamineacid/PSf, polyvinylamineacid/Na-exchanged MT/PSf, and AMT/PSf membranes is compared in Figures S12 and S13. The much higher CO_2 permeance and permselectivity of AMT/PSf membranes was ascribed to high-speed CO_2 transport channels in the AMT layer. While gas transport occurs mainly through the Na-exchanged MT interlayer gaps in the polyvinylamineacid/Na-exchanged MT/PSf membrane, the longer pathway that is due to the random orientation of Na-exchanged MT and the higher transport resistance owing to the presence of a continuous phase of polyvinylamineacid results in a lower gas permeance and permselectivity than for the AMT/PSf membrane. The modified PSf substrate membrane displays the highest CO_2 permeance but very low selectivity owing to the large mean pore diameter of the PSf porous membrane (45 nm; Figure S14, see the Supporting Information for further details).

The CO_2 permeability and selectivity of AMT/PSf and RMT/PSf membranes tested with dried mixed gases are compared with those reported in the literature in Figure 6 and Table S1. The Robeson upper-bound plots are intended to apply to single-gas permeability and ideal selectivity in purely polymeric membranes, but it is convenient and common practice to plot other types of membranes (e.g., polymeric mixed-matrix membranes) to visualize comparative performance. Figure 6 shows that the CO_2 permeability and selectivity of the AMT/PSf membrane for CO_2/N_2 and CO_2/CH_4 gas mixtures are above the Robeson 2008 upper bounds,[11] and for the CO_2/H_2 gas pair, they are far above the upper bound proposed by Freeman and co-workers.[12] Compared with other membranes, the AMT/PSf membrane displays a higher CO_2/CH_4 separation performance, and

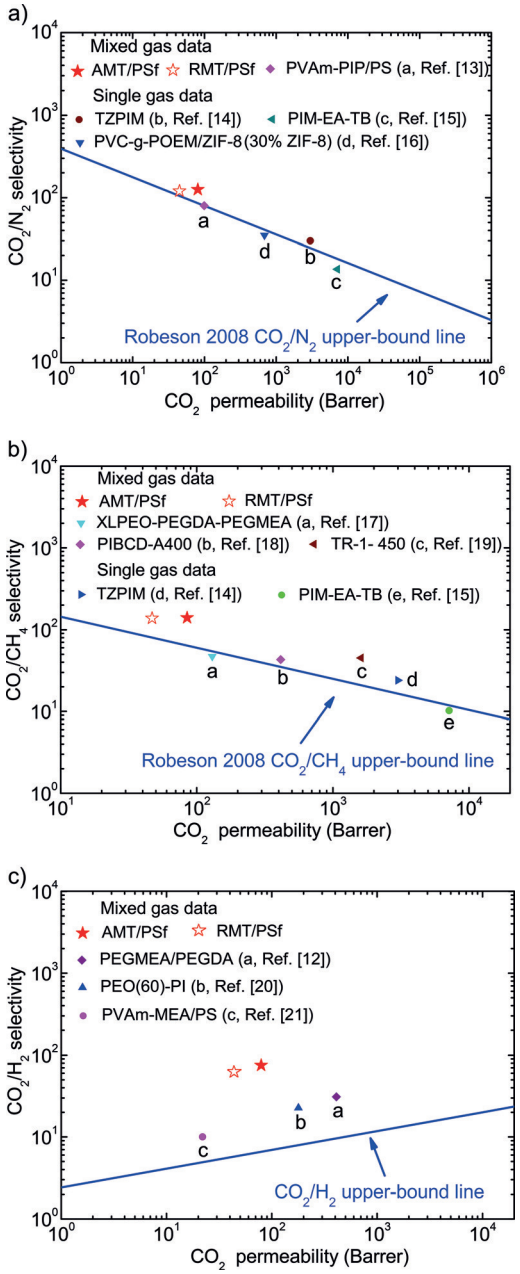

Figure 6. Mixed-gas separation of CO_2 with the AMT/PSf membrane compared with that of RMT/PSf and other polymeric and mixed-matrix membranes reported in the literature, tested using dry gases.[13–21]

a much higher CO_2/H_2 separation performance in particular (see the Supporting Information).

In an environment containing water vapor, the AMT interlayer gaps contain Na and K ions and water molecules (Figure S15). XRD analysis indicated that water molecules have no effect on the structural integrity of AMT, but result in a widening of the interlayer space to 0.96 nm (Figure S16). In the presence of water in the feed gas, the gas-transport channels broaden, but conversely, the CO_2 diffusion coefficient in the AMT interlayer gaps decreases. These two opposing effects result in an almost unchanged CO_2 separation performance of the AMT/PSf membrane at 50 °C when the amount of water vapor in the feed gas is varied (Table S2, Figure S17, and further details in the Supporting Information). It is of great significance that the CO_2 separation performance of the AMT/PSf membrane is independent of the feed pressure at 50 °C, and it maintains stable behavior with time. The results indicate that even if trace amounts of Ca ions remain in the interlayer gaps, they would not affect the long-term stability of the CO_2 separation performance of the AMT/PSf membrane. Tensile measurements and creep tests also indicate that the AMT/PSf membrane has excellent mechanical stability and high CO_2 separation performance below a creep-test pressure of 10.0 MPa (Table S3, Figures S18 and S19, and further details in the Supporting Information).

In summary, AMT/PSf mixed-matrix membranes containing aligned MT interlayer gaps as high-speed CO_2 transport channels have been prepared. Polyvinylamineacid interspersed and bonded with MT aligns and anchors the channels onto a PSf support membrane. The resulting AMT/PSf membranes display high CO_2 permeance and mixed-gas selectivities, and their performance is independent of the amount of water vapor in the gas feed. Thus the membranes may be useful for separation processes such as CO_2 capture from flue gas and CO_2 removal from natural gas and syngas. The present membrane fabrication method should be generally applicable for preparing other aligned clay membranes with interlayer gaps acting as gas transport channels. Hydroxy groups on the walls of other multilayered oxide clays should similarly facilitate interlayer gap alignment. When the interlayer gaps of aligned clay membranes are larger than that of the AMT membrane (0.88 nm), the gas diffusion coefficients increase, and therefore the aligned clay membranes may display higher CO_2 permeance and lower CO_2 selectivity than the present AMT membranes.

Acknowledgements

This research was supported by the Natural Science Foundation of China (20836006, 21436009), and the National High-tech Research and Development Project (2012AA03A611).

Keywords: carbon dioxide · gas separation · membranes · montmorillonite

How to cite: *Angew. Chem. Int. Ed.* **2016**, *55*, 9321 – 9325
Angew. Chem. **2016**, *128*, 9467 – 9471

[1] a) S. Li, J. L. Falconer, R. D. Noble, *Adv. Mater.* **2006**, *18*, 2601 – 2603; b) M. A. Carreon, S. Li, J. L. Falconer, R. D. Noble, *Adv. Mater.* **2008**, *20*, 729 – 732.
[2] G. P. Hao, W. C. Li, D. Qian, A. H. Lu, *Adv. Mater.* **2010**, *22*, 853 – 857.
[3] a) H. Lin, B. D. Freeman, *J. Mol. Struct.* **2005**, *739*, 57 – 74; b) L. Jiang, H. Chen, Y. C. Jean, T. S. Chung, *AIChE J.* **2009**, *55*, 75 – 86.
[4] a) M. Zhou, D. Korelskiy, P. Ye, M. Grahn, J. Hedlund, *Angew. Chem. Int. Ed.* **2014**, *53*, 3492 – 3495; *Angew. Chem.* **2014**, *126*, 3560 – 3563; b) T. H. Bae, J. S. Lee, W. Qiu, W. J. Koros, C. W. Jones, S. Nair, *Angew. Chem. Int. Ed.* **2010**, *49*, 9863 – 9866; *Angew. Chem.* **2010**, *122*, 10059 – 10062; c) S. R. Venna, J. B. Jasinski, M. A. Carreon, *J. Am. Chem. Soc.* **2010**, *132*, 18030 – 18033.
[5] a) O. Shekhah, J. Liu, R. A. Fischer, C. Wöll, *Chem. Soc. Rev.* **2011**, *40*, 1081 – 1106; b) H. Furukawa, K. E. Cordova, M. O'Keeffe, O. M. Yaghi, *Science* **2013**, *341*, 1230444.
[6] C. Wan, X. Qiao, Y. Zhang, Y. Zhang, *Polym. Test.* **2003**, *22*, 453 – 461.
[7] a) B. M. Choudary, M. L. Kantam, A. Rahman, C. V. Reddy, K. K. Rao, *Angew. Chem. Int. Ed.* **2001**, *40*, 763 – 766; *Angew. Chem.* **2001**, *113*, 785 – 788; b) R. K. Allada, A. Navrotsky, H. T. Berbeco, W. H. Casey, *Science* **2002**, *296*, 721 – 723; c) X. Guo, F. Zhang, D. G. Evans, X. Duan, *Chem. Commun.* **2010**, *46*, 5197 – 5210.
[8] X. Liu, X. Lu, M. Sprik, J. Cheng, E. J. Meijer, R. Wang, *Geochim. Cosmochim. Acta* **2013**, *117*, 180 – 190.
[9] a) M. Mulder, *Basic principles of membrane technology*, 2nd ed., Kluwer, Dordrecht, The Netherlands **1999**; b) A. B. Fuertes, *J. Membr. Sci.* **2000**, *177*, 9 – 16.
[10] C. Zhang, Z. Wang, Y. Cai, C. Yi, D. Yang, S. Yuan, *Chem. Eng. J.* **2013**, *225*, 744 – 751.
[11] L. M. Robeson, *J. Membr. Sci.* **2008**, *320*, 390 – 400.
[12] H. Lin, E. V. van Wagner, B. D. Freeman, L. G. Toy, R. P. Gupta, *Science* **2006**, *311*, 639 – 642.
[13] Z. Qiao, Z. Wang, C. Zhang, S. Yuan, Y. Zhu, J. Wang, S. Wang, *AIChE J.* **2013**, *59*, 215 – 228.
[14] N. Du, H. B. Park, G. P. Robertson, M. M. Dal-Cin, T. Visser, L. Scoles, M. D. Guiver, *Nat. Mater.* **2011**, *10*, 372 – 375.
[15] M. Carta, R. Malpass-Evans, M. Croad, Y. Rogan, J. C. Jansen, P. Bernardo, F. Bazzarelli, N. B. McKeown, *Science* **2013**, *339*, 303 – 307.
[16] W. K. Chi, S. J. Kim, S.-J. Lee, Y.-S. Bae, J. H. Kim, *ChemSusChem* **2015**, *8*, 650 – 658.
[17] H. Lin, E. van Wagner, R. Raharjo, B. D. Freeman, I. Roman, *Adv. Mater.* **2006**, *18*, 39 – 44.
[18] M. Chua, Y. Xiao, T.-S. Chung, *Chem. Eng. Sci.* **2013**, *104*, 1056 – 1064.
[19] H. B. Park, C. H. Jung, Y. M. Lee, A. J. Hill, S. J. Pas, S. T. Mudie, E. van Wagner, B. D. Freeman, D. J. Cookson, *Science* **2007**, *318*, 254 – 258.
[20] H. Chen, Y. Xiao, T.-S. Chung, *Polymer* **2010**, *51*, 4077 – 4086.
[21] Z. Qiao, Z. Wang, S. Yuan, J. Wang, S. Wang, *J. Membr. Sci.* **2015**, *475*, 290 – 302.

Received: April 1, 2016
Revised: May 16, 2016
Published online: June 17, 2016

